Structural dynamics inside a functionalized metal–organic framework probed by ultrafast 2D IR spectroscopy

Jun Nishida[a], Amr Tamimi[a], Honghan Fei[b], Sonja Pullen[c], Sascha Ott[c], Seth M. Cohen[b,1], and Michael D. Fayer[a,1]

[a]Department of Chemistry, Stanford University, Stanford, CA 94305; [b]Department of Chemistry and Biochemistry, University of California, San Diego, CA 92093; and [c]Department of Chemistry, Ångström Laboratory, Uppsala University, 75120 Uppsala, Sweden

Contributed by Michael D. Fayer, November 20, 2014 (sent for review November 4, 2014)

The structural elasticity of metal–organic frameworks (MOFs) is a key property for their functionality. Here, we show that 2D IR spectroscopy with pulse-shaping techniques can probe the ultrafast structural fluctuations of MOFs. 2D IR data, obtained from a vibrational probe attached to the linkers of UiO-66 MOF in low concentration, revealed that the structural fluctuations have time constants of 7 and 670 ps with no solvent. Filling the MOF pores with dimethylformamide (DMF) slows the structural fluctuations by reducing the ability of the MOF to undergo deformations, and the dynamics of the DMF molecules are also greatly restricted. Methodology advances were required to remove the severe light scattering caused by the macroscopic-sized MOF particles, eliminate interfering oscillatory components from the 2D IR data, and address Förster vibrational excitation transfer.

2D IR spectroscopy | metal–organic framework | UiO-66 MOF | ultrafast structural fluctuations | solvent confinement effect

Metal–organic frameworks (MOFs) are molecular architectures in which metal clusters are connected by organic linkers to yield relatively regular 3D coordination polymers with nanometer-sized pores (1, 2). MOFs have been investigated for a wide variety of chemical applications, such as adsorption of gases (3) and heterogeneous catalysts (4). Among many types of porous materials, MOFs are unique because of their structural elasticity coexisting with a high degree of spatial regularity. In some sense, MOFs are like crystals and polymers. They have relatively regular structures like a crystal, but the metal clusters are joined by organic linkers that, in some systems, produce significant structural mobility. The elasticity of MOFs is intimately related to their physical properties and behavior (5).

An important goal for understanding the nature of MOFs and how their chemical composition influences their properties and applications is to develop and apply an experimental method that can measure the ultrafast structural motions of MOFs. The relatively slow motions of the framework occurring in submicrosecond to millisecond scales have been studied by NMR and neutron scattering (6). However, until now, quantitative measurements that can characterize the time dependence of MOF structural motions in ultrafast regimes have not been possible because of the lack of appropriate techniques. Here, we have accomplished the goal by applying ultrafast 2D IR spectroscopy (7) to the study of MOF structural dynamics. 2D IR is akin to 2D NMR, but it operates on the ultrafast timescales necessary to characterize the time dependence of MOF structural motions. In addition, there is the important question of the effects on MOF dynamics when guest molecules fill the MOF nanopores. The guest molecules will affect the structural fluctuations of the framework by interacting with the linkers and the metal units. Furthermore, because of the confinement of guest molecules in MOF nanopores, the dynamics of these molecules are expected to be very different from their bulk liquid behavior (8). These issues can also be addressed with 2D IR spectroscopy.

The line shape observed in the FTIR absorption spectrum is related to the variety of environments that a vibrational probe experiences. The different environments produce a range of vibrational frequencies; this range of frequencies is called inhomogeneous broadening. Dynamics cause environments and therefore vibrational frequencies to change over time, but the time dependence of structural evolution cannot be extracted from the line shape. 2D IR experiments make the time evolution of the frequency of the vibrational probes and thus the time evolution of the structure a direct observable (9). The time-dependent evolution of the frequency is called spectral diffusion.

A useful way of thinking about the influence of environmental interactions on the frequencies of vibrational probe molecules is in terms of the electric field produced by the vibrational probes' surroundings (10). The atoms and molecular groups making up the environments around the vibrational probes have partial electrical charges. These partial charges produce a resultant electric field experienced by the probe vibration. The strength and direction of the electric field affect the vibrational frequency through the Stark effect. The vibrational probes that we study with 2D IR are chemically introduced into the MOFs. Because MOFs are not perfect crystals, the environment (electric field) experienced by different vibrational probe molecules will differ. Therefore, there will be a range of vibrational frequencies (the inhomogeneous broadening) that reflect the range of environments. The MOF structure is not static, and the metal clusters and the linkers are constantly moving. Relative to the vibrational probe, the distances and orientations of the various components

Significance

A unique aspect of metal–organic frameworks (MOFs) is their structural flexibility coexisting with a degree of regularity. Adsorbed guest molecules can cause MOF pore shapes to deform. Pore shape changes may be related to the high capacity and selectivity of the MOFs for gas adsorption and other processes. MOF flexibility and other properties are influenced by fast dynamics of the framework. Direct measurements to characterize fast motions of the MOFs have not been applied previously. We show that 2D IR spectroscopy can be performed on functionalized MOFs. We use 2D IR and other ultrafast IR methods to elucidate the timescales for ultrafast structural fluctuations and how they are influenced by a solvent filling the pores.

Author contributions: J.N., S.O., S.M.C., and M.D.F. designed research; J.N., A.T., H.F., and S.P. performed research; H.F., S.P., S.O., and S.M.C. contributed new reagents; J.N. and M.D.F. analyzed data; and J.N. and M.D.F. wrote the paper.

The authors declare no conflict of interest.

[1]To whom correspondence may be addressed. Email: scohen@ucsd.edu or fayer@stanford.edu.

This article contains supporting information online at www.pnas.org/lookup/suppl/doi:10.1073/pnas.1422194112/-/DCSupplemental.

in the framework that give rise to the electric field are changing. Thus, the frequency of each vibrational probe is time-dependent, and the time dependence of the frequencies of the vibrational probes (spectral diffusion) reflects the time dependence of the structural motions of the MOFs.

Recently, Pullen et al. (4) showed that a di-iron carbonyl complex [FeFe](dcbdt)$(CO)_6$ (dcbdt = 1,4-dicarboxylbenzene-2,3-dithiolate) can be incorporated into UiO-66 zirconium MOF as a linker in the framework (Fig. 1) (4). The CO stretching modes of the metal carbonyls have strong absorptions, which generate strong 2D IR signals (11). This complex was used as the vibrational probe to measure spectral diffusion. The CO modes have quite long vibrational relaxation lifetimes (~60 ps) which extend the temporal range of the dynamics observable with 2D IR spectroscopy.

To reach the goal of measuring the structural dynamics of MOFs with 2D IR spectroscopy, three major obstacles had to be overcome. First, the application of 2D IR spectroscopy to solid macroscopic particles like MOFs was problematic, because the MOFs scatter light excessively to an extent that can overwhelm the desired signal (12). Second, there are four IR active vibrational modes over a range of 100 cm^{-1} as shown in Fig. 1*B*. In the manner in which 2D IR vibrational echo spectroscopy is normally done, all four IR active modes are excited simultaneously by the IR laser pulses. The coherent excitation of all four modes produces very large oscillations of the time-dependent band shape in each of the 2D bands (13), making it almost impossible to extract the spectral diffusion induced by structural dynamics of the MOFs. Third, the spectral diffusion that we want to measure by 2D IR to obtain structural dynamics can also be caused by Förster vibrational excitation transfer among spatially nearby vibrational probes (14, 15). The 2D IR data by themselves cannot distinguish between these two spectral diffusion mechanisms. All of these problems were overcome to obtain the structural dynamics of the functionalized MOF by using 2D IR pulse-shaping techniques (12, 16, 17) and polarization-selective IR pump-probe experiments.

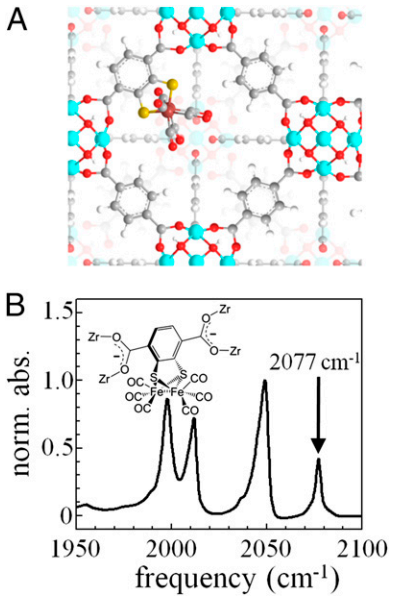

Fig. 1. (*A*) Structure of the functionalized UiO-66 MOF. Metal units ($[Zr_6(OH)_4O_4]$) are connected by 1,4-benzenedicarboxylate linkers to form octahedral nanopores. Some of the linkers are functionalized with the vibrational probe. (*B*) Linear IR absorption spectra for four IR active CO stretching modes of the functionalized UiO-66 MOF without solvent (dry). (*Inset*) Molecular structure of [FeFe](dcbdt)$(CO)_6$.

Results and Discussion

Functionalizing the MOF with the Vibrational Probe. The functionalized UiO-66 MOFs were prepared by postsynthetic exchange of the ligand component of the framework (4). UiO-66 was immersed in an aqueous solution of [FeFe](dcbdt)$(CO)_6$ at room temperature for 24 h. A schematic illustration of the MOF with a functionalized linker is shown in Fig. 1*A*. The loading of the functional group can be varied by changing the ratio of UiO-66 to [FeFe](dcbdt)$(CO)_6$ during the postsynthetic exchange reaction. Samples with the loadings of 14%, 2.5 ± 1.1%, and 0.2 ± 0.1% were prepared, where the loadings are expressed as the percentage of incorporated [FeFe](dcbdt)$(CO)_6$ compared with the total number of all linkers (Fig. S1 *A*–*C*). The MOFs were stored in a dry box with a humidity of <20 ppm, which is necessary to produce sufficiently dry MOFs for the studies (Fig. S1 *D* and *E*) (2).

2D IR Vibrational Echo Spectroscopy. In a 2D IR experiment, three excitation pulses impinge on the sample with controllable time delays. The nonlinear interaction of the three pulses with the vibrational probes generates a fourth pulse (the vibrational echo). The time between pulses 1 and 2 is τ, and the time between pulses 2 and 3 is T_w. The vibrational echo pulse is emitted at a time $\leq\tau$ after pulse 3.

The experimental details of 2D IR spectroscopy with pulse shaping have been previously described (17). A 160-fs IR pulse tuned to 2,070 cm^{-1} was separated into a strong pump pulse and a weak probe pulse. The pump pulse was introduced into the pulse-shaping system that converts the incoming pump pulse into two pump pulses (pulses 1 and 2) temporally separated by time τ. These two pump pulses label all of the vibrational oscillators with their initial frequencies. During the time period T_w, the structure of the MOF evolves. Then, pulse 3 generates the vibrational echo signal that reads out the frequencies of the vibrational oscillators after the system has had the period T_w to evolve. The vibrational echo signal propagates collinearly with pulse 3, which also serves as a local oscillator (LO) to detect the phase of the echo signal. The combined echo and LO are sent into a spectrograph, and the frequencies are detected on a 32-element IR array.

The 2D IR spectra require two Fourier transforms to go from the time domain to the frequency domain. The spectrograph performs one of the Fourier transforms experimentally by resolving the echo/LO pulse into its composite frequencies, giving the ω_m (vertical axis) of the 2D spectrum. The horizontal axis is obtained by scanning τ; when τ is scanned, the echo moves in time relative to the fixed LO, producing an interferogram. The interferogram recorded at each ω_m is numerically Fourier-transformed to give the ω_τ (horizontal axis) of the 2D spectrum (Fig. 2).

For each T_w, τ is scanned, and a 2D IR spectrum is obtained. The spectral diffusion (and thus, the structural evolution) is extracted from the evolution of the 2D band shape with respect to T_w. At short T_w, the detection frequency (ω_m) is approximately the same as the excitation frequency (ω_τ), giving a spectrum that is elongated along the diagonal. The shape of the spectrum becomes more symmetrical as spectral diffusion occurs, which causes the initial and final frequencies to be less correlated; the spectrum will be completely round when all structures have been sampled during the period T_w.

Fig. 2 *A* and *B* shows 2D IR spectra taken on the symmetric CO stretching mode of the MOF vibrational probe [FeFe](dcbdt)$(CO)_6$ at 2,077 cm^{-1} (the scattered light and oscillation suppression methods discussed below were used to take the data). Fig. 2*A* shows the 2D IR spectrum at relatively short time (2.5 ps). The red band in Fig. 2*A* is from 0 to 1 (ground state to first excited state) vibrational transition. Below, the blue band in Fig. 2*A* arises from the 1 to 2 vibrational transition. The dynamical information of interest here is contained in the 0 to 1

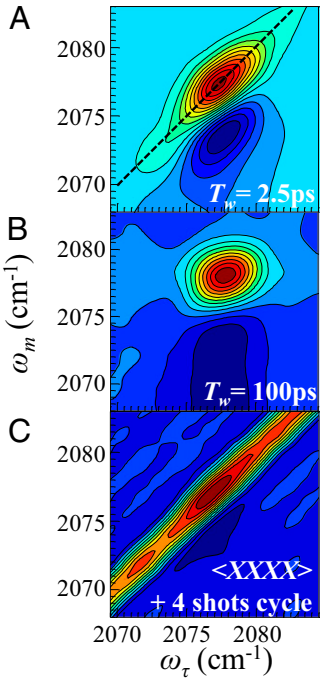

Fig. 2. (*A* and *B*) 2D IR spectra of the functionalized UiO-66 MOF (14% loading) at short time and long time taken with the scattering removal and the selective pumping schemes discussed in the text. The dashed line in *A* is the diagonal. The dynamical information is contained in the T_w-dependent shapes of the 2D IR spectra. (*C*) Data taken with standard polarizations and four-shots phase cycling. The spectrum is completely dominated by scattered light and not usable to obtain dynamical information.

band. The dashed line through the data in Fig. 2*A* is the diagonal. At short time, the spectrum is elongated along the diagonal, because there has been little spectral diffusion. Fig. 2*B* shows the spectrum at long time (100 ps). It is clear that the shape has changed substantially and the band is almost round, indicating that diffusion is almost complete by 100 ps.

To quantitatively extract the dynamical information, the center line slope (CLS) method was used (9). The CLS analysis provides a decay curve that contains the time constants and relative amplitudes of the components of the spectral diffusion. The CLS has been theoretically shown to be proportional to the frequency–frequency correlation function (FFCF). The absolute FFCF can be obtained from the CLS and the linear absorption spectrum as previously described (9).

Scattering Removal and Coherent Oscillation Suppression Methods. As mentioned above, one of the main obstacles to performing 2D IR experiments on an MOF powder is severe light scattering. The dominant interference with the signal is scatter from the pump pulses that is heterodyned by the probe beam. Shim et al. (12) showed that such contamination can be removed by a four-shot phase-cycling scheme. For a given τ, the phases of the two pump pulses (pulses 1 and 2) are varied to have relative phases $(0, 0)$, $(0, \pi)$, $(\pi, 0)$, and (π, π). This approach is useful for a sample that produces reasonably small amounts of scattered light.

We applied the four-shot phase-cycling sequence to the functionalized UiO-66 MOF dry powder to probe the symmetric stretching mode at 2,077 cm^{-1} (Fig. S2). The standard polarizations (<*XXXX*>) were used, in which the three input pulses and the detected echo pulse all had the same horizontal polarizations. This polarization scheme produces the largest signal. The result is shown in Fig. 2*C*. Scattered light is manifested as a large amplitude band along the diagonal that is overwhelming a resonant signal from the vibrational probe. As discussed in *SI Text*, the four-shot phase cycle does not eliminate scattered light from pulse 1 heterodyning with scattered light from pulse 2. To eliminate this problem, the pulse sequence is changed in two ways. First, the pump pulses 1 and 2 polarizations are rotated to vertical. Although this polarization scheme (<*XXYY*>) reduces the echo signal by a factor of ~3 (18), it eliminates the contamination from the scattered pump beams by a factor of >300. Second, an eight-shot cycle is used, in which pulse 3, the probe pulse, is chopped every other shot. The 2D IR spectra in Fig. 2 *A* and *B* were both taken with this scattering removal scheme. The scattered light artifacts are eliminated, which permits the accurate determination of the time evolution of the 2D IR spectrum. The same polarizations and phase-cycling pulse sequence was recently used in a different application (2D IR microscopy) (19).

With the scattered light artifacts eliminated, we can take high-quality 2D IR data, which are analyzed and plotted as CLS decays. The second major problem is the broad spectrum of the short pulses that excite all four IR active modes of the vibrational probe (Fig. 1*B*). Fig. 3*A* shows the spectrum of pump pulses 1 and 2 (Fig. 3*A*, black curve). Fig. 3*B* shows the first few picoseconds of the CLS data taken with the full pump spectrum (Fig. 3*B*, black circles and dashed curve). The large oscillations are caused by the coherent excitation of all four modes (Figs. S3 and S4) (13). The oscillations continue well past 10 ps, which interferes with the extraction of the CLS decay measurement of spectral diffusion. The Fourier transform of these oscillations gives the modes' frequency splittings (Fig. S3*C*).

To eliminate the oscillations, the pulse shaper was used to modify the spectrum of the IR pulses 1 and 2 as shown as the red curve in Fig. 3*A*. The change in the spectrum reduces the time resolution of the experiments, but the resulting time resolution is still more than sufficient to measure the spectral diffusion (*SI Text* and Fig. S5). By using the modified spectrum, the symmetric

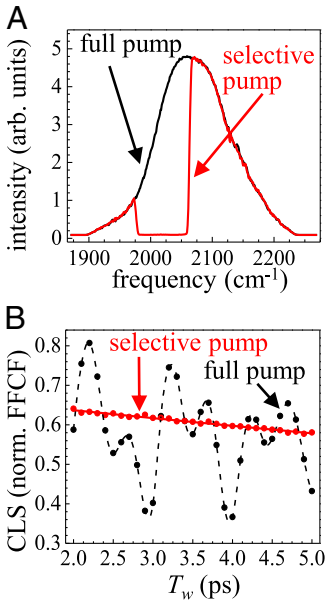

Fig. 3. (*A*) Spectra of IR pulses 1 and 2 in the vibrational echo pulse sequence. Black shows the full laser spectrum. Red shows the spectrum modified by the pulse shaper to give the selective pump that only excites the desired symmetric CO stretch. (*B*) CLS decay extracted from the 2D IR spectra for the 2.5% loading sample. The data taken with the full laser spectrum (black points and curve) display large-amplitude oscillations. In the data taken with the selective pump (red points and curve), the oscillations are eliminated.

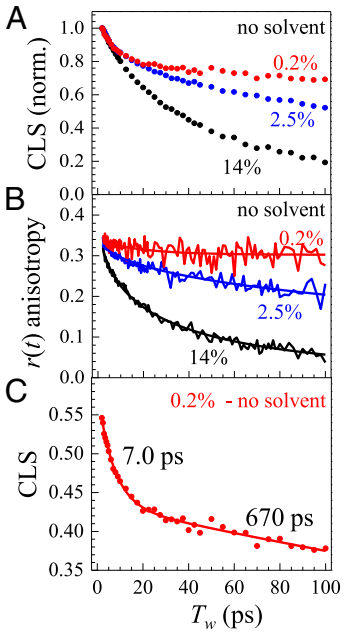

Fig. 4. (*A*) CLS data (normalized) obtained from time-dependent 2D IR spectra for three vibrational probe concentrations showing the substantial concentration dependence of the decays. (*B*) The anisotropy decay measured by IR pump-probe experiments for three concentrations. The change with concentration shows that the higher concentrations have substantial Förster vibrational excitation transfer. The 0.2% sample is free of excitation transfer. (*C*) The CLS decay for the 0.2% sample arises from MOF structural fluctuations.

stretching mode is selectively excited by the pump pulses. The red circles and curve in Fig. 3*B* are the short time portion of the CLS data taken with the modified pump pulses. As is clear from Fig. 3*B*, the oscillations are eliminated, and it is now possible to measure the desired CLS decay.

MOF Dynamics Without Solvent. Two of three hurdles that must be overcome to reach our goal of measuring MOF dynamics have now been dealt with. We can obtain high-quality 2D IR dynamical data without interference from scattered light or CLS oscillations. Data were taken on dry (no solvent or absorbed water) functionalized MOFs with vibrational probe loadings of 14%, 2.5%, and 0.2%. Fig. 4*A* shows CLS decays for three types of samples. Clearly, the loading strongly influences the decays. For 14% loading, one in seven linkers has a vibrational probe. This loading puts the vibrational probes very close together, which can result in Förster vibrational excitation transfer (14, 15). If a vibrational excitation starts on one vibrational probe that has a certain vibrational frequency and it hops to another probe with a different frequency, the result is a time-dependent change in the frequency. The change in frequency is excitation transfer-induced spectral diffusion (ETISD), which is distinct from structural spectral diffusion caused by the structural evolution of the system. The rate of Förster transfer decreases as $1/R^6$, where R is the distance between vibrational probes. The highly concentration-dependent decays in Fig. 4*A* indicate that ETISD may be involved as a spectral diffusion mechanism.

When an excitation hops from one vibrational probe to another, in general, the transition dipoles of the two probes will point in different directions. Therefore, excitation hopping results in changes of the transition dipole directions of the excited vibrational probes. This process can be investigated using polarization-selective IR pump-probe experiments. The anisotropy decay, $r(t)$, was obtained by measuring the IR pump-probe signal with the probe polarization parallel $[S_{\parallel}(t)]$ and perpendicular $[S_{\perp}(t)]$ to the pump polarization, with $r(t) = [S_{\parallel}(t) - S_{\perp}(t)]/[S_{\parallel}(t) + 2S_{\perp}(t)]$ (18). The initial excitation of vibrational probes tends to be along the direction of the electric field of the IR pump pulse. Excitation transfer causes the initial distribution of angles to become random. As a result, the anisotropy $[r(t)]$ will decay in time (20, 21). The anisotropy decay can be induced by the physical reorientation of the vibrational probe as well (orientational relaxation). However, in the MOFs, the vibrational probe is rigidly bonded to the linker and can undergo, at most, very restricted small-angle orientational relaxation.

Fig. 4*B* shows the anisotropy decays for three samples. Note that these data were taken with the selective pumping scheme described above (Fig. 3*A*). The 14% and 2.5% samples have substantial decays. However, the 0.2% sample has a very small amount of decay at short time, and then, the anisotropy curve becomes horizontal, which indicates that there is no additional anisotropy decay. This small amplitude decay to a constant plateau is consistent with the well-known wobbling-in-a-cone orientational relaxation, in which probes have restricted angular motions (22). They can sample a limited range of angles, namely the cone. After they have sampled this restricted range of angles, there is no additional decay of the anisotropy.

Because orientational relaxation is not concentration-dependent, the anisotropy decays of the 14% and 2.5% samples are attributed to excitation transfer. This conclusion is further supported by the fact that the anisotropy decays for 14% and 2.5% samples were fit well in the form of $Ae^{-(t/\tau_{ET})^{1/2}}$, which describes the excitation transfer-induced anisotropy decay in systems with transition dipoles that have random orientations and separations (23). The solid curves in Fig. 4*B* through the 14% and 2.5% data are fits to this function. In the UiO-66 MOFs, there is a large variety of angles and distances, making $Ae^{-(t/\tau_{ET})^{1/2}}$ a useful approximation. As the probe loading is reduced (2.5%), the anisotropy decay is slower, because the average separation between vibrational probes is increased, and the excitation transfer slows down; τ_{ET} is inversely proportional to the square of the loading. The τ_{ET} for the 2.5% is, indeed, slower by the square of the ratio of the concentrations within experimental error (Fig. S6). Thus, the source of the spectral diffusion in Fig. 4*A* for the 14% and 2.5% samples is ETISD. When the concentration is further reduced to 0.2%, we calculate τ_{ET} to be longer than 50 ns. Therefore, excitation transfer is negligible in the 0.2% sample. The solid curve through the 0.2% sample is a single exponential decay with a constant offset. Therefore, for the 0.2% sample, both the anisotropy decay and the spectral diffusion are not contaminated by vibrational excitation transfer. The initial decay in the anisotropy of the 0.2% sample is caused by the wobbling motion of the probe. The wobbling cone angle and wobbling time constant can be extracted using the wobbling-in-a-cone theory (24). The total cone half-angle, including inertial and diffusive wobbling, is 24°, with the wobbling time constant of 18 ± 6 ps (Table 1).

Table 1. Dynamical parameters from polarization-selective pump-probe experiments on MOFs

Sample	τ_{r1} (ps)	τ_{r2} (ps)	$r(0)$	$r(\infty)$	θ_{int} (°)	θ_{cone} (°)	τ_w (ps)
0.2% (dry)	5.2	61	0.34	0.30	19	24	18 ± 6
0.2% (DMF)	3.8	43	0.34	0.30	19	25	42 ± 21

τ_{r1} and τ_{r2} are the vibrational relaxation time constants obtained by a biexponential fit of the population decay. The faster component is caused by the equilibration of the vibrational population among four vibrational modes. $r(0)$ and $r(\infty)$ are the initial value and the long-time offset in the anisotropy decay, respectively. θ_{int} and θ_{cone} are the inertial and wobbling cone angles extracted from $r(0)$ and $r(\infty)$, respectively. τ_w is the wobbling time constant. Details are in *SI Text*.

Table 2. 2D IR FFCF parameters on MOFs and bulk solution

Sample	ν_{peak} (cm^{-1})	Δ_{tot} (cm^{-1})	Γ (cm^{-1})	Δ_1 (cm^{-1})	τ_1 (ps)	Δ_2 (cm^{-1})	τ_2 (ps)
0.2% (dry)	2,077.0	3.2	0.41	1.5	7.0 ± 0.5	2.7	670 ± 50
0.2% (DMF)	2,071.4	5.4	1.0	2.0	23 ± 7	4.4	>2,000
Bulk DMF	2,078.9	5.2	4.2	2.4	16 ± 1	—	—

ν_{peak} is the peak position of the symmetric stretching mode. Δ_{tot} is the total line width of the absorption band. Γ is the Lorentzian homogeneous line width. Δ_1 and Δ_2 are amplitudes (inhomogeneous Gaussian line width components) for the faster and slower dynamical processes, respectively. τ_1 and τ_2 are spectral diffusion time constants for faster and slower dynamical processes, respectively. All of the line widths are given in full-width at half-maximum. The total line width is the convolution of the two Gaussian inhomogeneous components, which is then convolved with the Lorentzian homogeneous component.

The problem of ETISD is eliminated by examining the 0.2% sample. The CLS decay for this sample, which reports on the structural spectral diffusion, is displayed in Fig. 4*C* without normalization (Fig. 4*C*, red circles). The solid red curve in Fig. 4*C* is a biexponential fit to the CLS data. The CLS together with a linear absorption spectrum permit the full FFCF to be obtained, including the homogeneous contribution to the total line width (9). The parameters are given in Table 2. The spectral diffusion time constants are $\tau_1 = 7$ ps and $\tau_2 = 670$ ps. The slow component amplitude ($\Delta_2 = 2.7$ cm^{-1}) is approximately two times that of the fast component ($\Delta_1 = 1.5$ cm^{-1}). The observed spectral diffusion is too slow to be induced by the intramolecular vibrations of the probe (Fig. 1*B*, *Inset*) and is attributed to a larger-scale motion of the MOF framework. There are at least two types of framework structural fluctuations that are likely to contribute to the observed spectral diffusion. The wobbling of the probe shows that the framework is undergoing undulatory motions that can involve many MOF unit cells. MOFs can also have breathing motions, in which each unit cell expands, contracts, and changes shape in a concerted manner (25). The characteristic time constants for these structural fluctuations are the spectral diffusion time constants. In addition, there is an ultrafast motionally narrowed homogeneous contribution to the line width: $\Gamma = 0.41$ cm^{-1}. These ultrafast motions can arise from vibrations of small groups, including the vibrational probe, on a sub–100-fs timescale.

UiO-66 MOF is considered to be relatively rigid (2), and it is important that, even in a rigid MOF, there is fast structural evolution. Because the measurements were only made to 100 ps (because of the finite vibrational lifetime), we cannot rule out the possibility that an even slower process with relatively low amplitude exists. If there is a very slow component, the 7-ps decay time is not affected, but slow component fit (670 ps) would become somewhat faster. It is also possible that there is nonevolving structural inhomogeneity in the UiO-66 framework. Recently, several studies have indicated that UiO-66 MOF, in particular, has more linker defects (missing linkers) than other types of MOFs (26), potentially leading to a static local inhomogeneity, which would produce an offset at very long time in the CLS decay.

Effect of Dimethylformamide in MOF Pores on the Dynamics. The 2D IR and IR pump-probe experiments were also performed on the 0.2% loading sample immersed in dimethylformamide (DMF). On the immersion in DMF, the absorption peak position of the CO symmetric stretching mode shifted to ~2,071.5 cm^{-1} from 2,077 cm^{-1} for the dry sample (Fig. S2), and the line width Δ_{tot} was significantly broadened (Table 1). Also, the vibrational relaxation lifetime was reduced to 40 ps from 60 ps (Fig. S7 and Table S1). These observations show that the vibrational probes are in close contact with DMF molecules, and thus, the DMF molecules are absorbed into the framework pores.

The CLS decay of the 0.2% sample in DMF is plotted in Fig. 5. For comparison, the CLS decay for the 0.2% with no solvent is also plotted (expanded view in Fig. S8). In addition, the analog of the vibrational probe that is lacking the carboxylate groups, [FeFe](bdt)$(CO)_6$ (bdt = benzene-1,2-dithiolate), was dissolved in bulk DMF as a 3.3 mM solution, and the CLS decay was measured in the same manner as used for the MOF samples. The dynamical parameters extracted from the CLS decays are given in Table 2. It is clear from Fig. 5 that the addition of DMF to the MOF pores slowed the structural dynamics of the MOF. The fast component slowed from 7 ps to 23 ps, and the 670-ps slow component without solvent became too slow to measure (Table 2). In contrast, the vibrational probe analog [FeFe](bdt)$(CO)_6$ dissolved in bulk DMF has an enormous homogeneous component, and the spectral diffusion is a single exponential decay with a 16-ps time constant. The very large homogeneous width is caused by ultrafast motions of the bulk DMF molecules. These ultrafast solvent motions are dominant dynamics experienced by the vibrational probe analog in bulk DMF. The minor inhomogeneous component undergoes complete spectral diffusion with the 16-ps time constant.

Filling the MOF pores with DMF has a major impact on the structural dynamics of both the MOF and DMF. The MOF structural evolution is substantially slower when the pores are filled with DMF. The slowing may be rationalized as arising from resistance to pore structural fluctuations because of the need for the DMF molecules in the pores to respond to motions of the framework. Framework fluctuations that change both shape and volume of the pores are inhibited by DMF inside the pores. In addition, ultrafast motions of DMF are suppressed in the pores as shown by the large difference in the homogeneous line widths of the probe when it experiences DMF in the pores vs. the bulk solution (Table 2). The slowing of DMF dynamics in nanometer-sized pores is consistent with slowing of dynamics in other nanoscopically confined systems, such as water in small reverse micelles (8, 27). There are several molecular dynamics simulations indicating that guest molecules adsorbed in some MOFs experience strong confinement effects (28) and that the adsorbed molecules strongly interact with the organic linkers to potentially enhance

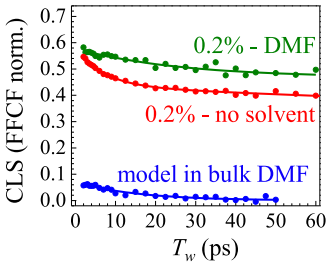

Fig. 5. Comparison of CLS decays (structural spectral diffusion) for the MOF with no solvent, the MOF with MOF pores filled with DMF, and the vibrational probe analog [FeFe](bdt)$(CO)_6$ in bulk DMF.

the rigidity of the framework (29). The 2D IR results provide experimental support for the simulation results.

Concluding Remarks

The main results of this study are the measurement with 2D IR of the UiO-66 MOF structural dynamics. With no solvent, dynamical time constants of 7 and 670 ps are obtained. The MOF structural dynamics slow substantially when the pores were filled with DMF, and the adsorbed DMF dynamics are drastically different from those of bulk DMF liquid. The measurements were made possible by the elimination of scattered light (Fig. 2), the elimination of interfering oscillations in the data (Fig. 3), and the elimination of Förster excitation transfer (Fig. 4*B*). UiO-66 is considered to be a fairly rigid MOF; nonetheless, there are substantial dynamics on the 10-ps and subnanosecond timescales. These structural fluctuations sample all or a large fraction of the structural configurations that give rise to the vibrational probe's inhomogeneously broadened absorption line.

An intriguing aspect of some MOFs is their ability to change lattice structure on the introduction of a solvent into the pores (5). This property is sometimes referred to as flexibility (25, 30). In some sense, this deformation is similar to a crystal lattice phase transition, in which, for example, a lattice changes from monoclinic to triclinic when temperature is changed. In a crystal lattice-phase transition, certain lattice modes are intimately involved in the transition. As the transition temperature is approached from above, the modes that move the lattice components into configurations that resemble the new phase have increased amplitude and reduced frequency (31). For MOFs, structural changes can be driven by interactions with the solvent rather than a change in temperature. It will be interesting and important to study flexible MOFs with 2D IR and observe changes in the structural fluctuations with various solvent loadings as the MOF structural transition is approached and occurs. Such experiments have the potential to explicate the connection between structural dynamics and solvent-induced structural transitions.

Materials and Methods

Sample Preparation. Functionalized UiO-66 MOFs are synthesized as reported in ref. 4. The details can be found in *SI Text*. DMF used for the dynamical studies was obtained from Sigma Aldrich and used without additional purifications.

2D IR Spectroscopy/Polarization-Selective Pump-Probe Spectroscopy. The output of a Ti:Sapphire regenerative amplifier with a pulse energy of ~680 μJ, duration of ~100 fs, and repetition rate of 1 kHz was used to pump a near-IR optical parametric amplifier followed by difference frequency generation to yield ~8-μJ IR pulses with ~160-fs duration centered at ~2,070 cm^{-1}. A detailed description for the pulse-shaping system used in this study can be found in ref. 17. In polarization-selective pump-probe spectroscopy, the polarizations of the pump and probe beams were set to 45° and 0°, respectively. The probe beam was resolved after the sample to either +45° (parallel) or −45° (perpendicular) by a polarizer on a computer-controlled rotator, sent through a polarizer fixed to 0° into the spectrograph, and detected by a 32-element array detector. The anisotropy decays reported in Fig. 4*B* are those at the center frequency of the 0–1 transition (2,077 cm^{-1}).

ACKNOWLEDGMENTS. J.N. and A.T. acknowledge support from Stanford Graduate Fellowships. This work was funded by Division of Chemical Sciences, Geosciences, and Biosciences, Office of Basic Energy Sciences of the US Department of Energy (DOE) Grant DE-FG03-84ER13251, which partially supported M.D.F., materials, and supplies and contributed to support of the instrumentation. Air Force Office of Scientific Research (AFOSR) Grant FA9550-12-1-0050 also partially supported M.D.F. and contributed to the development and support of the instrumentation. When not supported by fellowships, J.N. was supported by the AFOSR, and A.T. was supported by the DOE. The contributions of H.F. and S.M.C. to the research were supported by National Science Foundation, Division of Materials Research Grant DMR-1262226. The contributions of S.P. and S.O. to the research were supported by the Swedish Research Council, the Swedish Energy Agency, and the Knut and Alice Wallenberg Foundation.

1. Li H, Eddaoudi M, O'Keeffe M, Yaghi OM (1999) Design and synthesis of an exceptionally stable and highly porous metal-organic framework. *Nature* 402(6759): 276–279.
2. Cavka JH, et al. (2008) A new zirconium inorganic building brick forming metal organic frameworks with exceptional stability. *J Am Chem Soc* 130(42):13850–13851.
3. Li JR, Kuppler RJ, Zhou HC (2009) Selective gas adsorption and separation in metal-organic frameworks. *Chem Soc Rev* 38(5):1477–1504.
4. Pullen S, Fei H, Orthaber A, Cohen SM, Ott S (2013) Enhanced photochemical hydrogen production by a molecular diiron catalyst incorporated into a metal-organic framework. *J Am Chem Soc* 135(45):16997–17003.
5. Horike S, Shimomura S, Kitagawa S (2009) Soft porous crystals. *Nat Chem* 1(9): 695–704.
6. Kolokolov DI, et al. (2012) Probing the dynamics of the porous Zr terephthalate Uio-66 framework using ^{2}H NMR and neutron scattering. *J Phys Chem C* 116(22): 12131–12136.
7. Park S, Kwak K, Fayer MD (2007) Ultrafast 2D-IR vibrational echo spectroscopy: A probe of molecular dynamics. *Laser Phys Lett* 4(10):704–718.
8. Fayer MD (2012) Dynamics of water interacting with interfaces, molecules, and ions. *Acc Chem Res* 45(1):3–14.
9. Kwak K, Park S, Finkelstein IJ, Fayer MD (2007) Frequency-frequency correlation functions and apodization in two-dimensional infrared vibrational echo spectroscopy: A new approach. *J Chem Phys* 127(12):124503.
10. Williams RB, Loring RF, Fayer MD (2001) Vibrational dephasing of carbonmonoxy myoglobin. *J Phys Chem B* 105(19):4068–4071.
11. Rosenfeld DE, Gengeliczki Z, Smith BJ, Stack TDP, Fayer MD (2011) Structural dynamics of a catalytic monolayer probed by ultrafast 2D IR vibrational echoes. *Science* 334(6056):634–639.
12. Shim SH, Strasfeld DB, Ling YL, Zanni MT (2007) Automated 2D IR spectroscopy using a mid-IR pulse shaper and application of this technology to the human islet amyloid polypeptide. *Proc Natl Acad Sci USA* 104(36):14197–14202.
13. Wong DB, Giammanco CH, Fenn EE, Fayer MD (2013) Dynamics of isolated water molecules in a sea of ions in a room temperature ionic liquid. *J Phys Chem B* 117(2): 623–635.
14. Cowan ML, et al. (2005) Ultrafast memory loss and energy redistribution in the hydrogen bond network of liquid H_2O. *Nature* 434(7030):199–202.
15. Rosenfeld DE, Fayer MD (2012) Excitation transfer induced spectral diffusion and the influence of structural spectral diffusion. *J Chem Phys* 137(6):064109.
16. Middleton CT, Woys AM, Mukherjee SS, Zanni MT (2010) Residue-specific structural kinetics of proteins through the union of isotope labeling, mid-IR pulse shaping, and coherent 2D IR spectroscopy. *Methods* 52(1):12–22.
17. Karthick Kumar SK, Tamimi A, Fayer MD (2012) Comparisons of 2D IR measured spectral diffusion in rotating frames using pulse shaping and in the stationary frame using the standard method. *J Chem Phys* 137(18):184201.
18. Tao T (1969) Time-dependent fluorescence depolarization and Brownian rotational diffusion coefficients of macromolecules. *Biopolymers* 8(5):609–632.
19. Baiz CR, Schach D, Tokmakoff A (2014) Ultrafast 2D IR microscopy. *Opt Express* 22(15): 18724–18735.
20. Woutersen S, Bakker HJ (1999) Resonant intermolecular transfer of vibrational energy in liquid water. *Nature* 402(6761):507–509.
21. Chen H, Wen X, Li J, Zheng J (2014) Molecular distances determined with resonant vibrational energy transfers. *J Phys Chem A* 118(13):2463–2469.
22. Lipari G, Szabo A (1980) Effect of librational motion on fluorescence depolarization and nuclear magnetic resonance relaxation in macromolecules and membranes. *Biophys J* 30(3):489–506.
23. Peterson KA, Zimmt MB, Linse S, Domingue RP, Fayer MD (1987) Quantitative determination of the radius of gyration of poly(methyl methacrylate) in the amorphous solid state by time-resolved fluorescence depolarization measurements of excitation transport. *Macromolecules* 20(1):168–175.
24. Tan HS, Piletic IR, Fayer MD (2005) Orientational dynamics of water confined on a nanometer length scale in reverse micelles. *J Chem Phys* 122(17):174501.
25. Férey G, Serre C (2009) Large breathing effects in three-dimensional porous hybrid matter: Facts, analyses, rules and consequences. *Chem Soc Rev* 38(5):1380–1399.
26. Wu H, et al. (2013) Unusual and highly tunable missing-linker defects in zirconium metal-organic framework UiO-66 and their important effects on gas adsorption. *J Am Chem Soc* 135(28):10525–10532.
27. Moilanen DE, Fenn EE, Wong D, Fayer MD (2009) Water dynamics in large and small reverse micelles: From two ensembles to collective behavior. *J Chem Phys* 131(1): 014704.
28. Medders GR, Paesani F (2014) Water dynamics in metal-organic frameworks: Effects of heterogeneous confinement predicted by computational spectroscopy. *J Phys Chem Lett* 5(16):2897–2902.
29. Grosch JS, Paesani F (2012) Molecular-level characterization of the breathing behavior of the jungle-gym-type DMOF-1 metal-organic framework. *J Am Chem Soc* 134(9): 4207–4215.
30. Wang Z, Cohen SM (2009) Modulating metal-organic frameworks to breathe: A postsynthetic covalent modification approach. *J Am Chem Soc* 131(46):16675–16677.
31. Dougherty TP, et al. (1992) Femtosecond resolution of soft mode dynamics in structural phase transitions. *Science* 258(5083):770–774.